Morphometric analysis of the infratemporal fossa using three-dimensional (3D) digital models

Erdem, Huseyin; Cevik, Yigit; Safak, Nazire Kilic; Soames, Roger W.; Pehlivan, Umur Anil; Boyan, Neslihan

Published in:
Surgical and Radiologic Anatomy

DOI:
10.1007/s00276-023-03144-5

Publication date:
2023

Document Version
Peer reviewed version

Morphometric Analysis of the Infratemporal Fossa Using Three-Dimensional (3D) Digital Models

Huseyin Erdem[1], Yigit Cevik[1], Nazire Kilic Safak[1], Roger W. Soames[2], Umur Anil Pehlivan[3], Neslihan Boyan[1], Ozkan Oguz[1]

[1] Department of Anatomy, Faculty of Medicine, Cukurova University, Adana, Turkey, 01330

[2] Centre for Anatomy and Human Identification, School of Science and Engineering, University of Dundee, Dundee, UK, DD14HN

[3] Department of Radiology, Baskent University Hospital Adana, Adana, Turkey, 01330

Huseyin Erdem, Department of Anatomy, Faculty of Medicine, Cukurova University, Adana, Turkey, 01330, ORCID: 0000-0002-7746-7464

Yigit Cevik, Department of Anatomy, Faculty of Medicine, Cukurova University, Adana, Turkey, 01330, ORCID: 0000-0002-2691-3284

Nazire Kilic Safak, Department of Anatomy, Faculty of Medicine, Cukurova University, Adana, Turkey, 01330, ORCID: 0000-0003-1521-5437

Roger W. Soames, Centre for Anatomy and Human Identification, School of Science and Engineering, University of Dundee, Dundee, UK, DD14HN, ORCID: 0000-0003-1359-172X

Umur Anil Pehlivan, Department of Radiology, Baskent University Hospital Adana, Adana, Turkey, 01330, ORCID: 0000-0001-5871-0695

Neslihan Boyan, Department of Anatomy, Faculty of Medicine, Cukurova University, Adana, Turkey, 01330, ORCID: 0000-0001-9524-9535

Ozkan Oguz, Department of Anatomy, Faculty of Medicine, Cukurova University, Adana, Turkey, 01330, ORCID: 0000-0002-3081-1467

Corresponding author:

Huseyin Erdem, Ph.D.

Department of Anatomy, Faculty of Medicine,

Cukurova University, Adana, Turkey, 01330

e-Mail: herdem@cu.edu.tr

Acknowledgments: The authors sincerely thank to technical staff of the Cukurova University Department of Radiology for their technical support and contribution to the collection of CT dataset.

Abstract

Purpose: The infratemporal fossa contains important neurovascular components and is directly related to other anatomical regions and structures. The morphometric distances between the bones forming its borders have not been thoroughly investigated. The aim of this study was to determine the morphometry of the infratemporal fossa.

Methods: 3D models of the skull of 83 individuals were reconstructed from DICOM datasets, from which length, depth and width measurements were determined and compared between genders and the right and left sides.

Results: All measurements obtained were significantly different between males and females. There were also significant differences between the left and right sides for depth and width measurements.

Conclusion: This is the first study to determine and investigate measurements of the infratemporal fossa; as such it provides a comprehensive view of the morphology of the fossa. It provides valuable information for surgical interventions and differential diagnoses of pathologies in this region, as well as enhancing its understanding in medical education.

Keywords: 3D analysis, infratemporal fossa, morphometric analysis, skull base, three-dimensional reconstruction.

Introduction

The infratemporal fossa is an important irregular anatomical region/space below the skull base: it approximates an inverted pyramidal-shaped cavity between the styloid process of the temporal bone and posterior surface of the maxillary sinus. It is bounded by the zygomatic arch, mandibular ramus, lateral pterygoid plate, and greater wing of the sphenoid [3]. The region contains a number of important anatomical structures: otic ganglion, chorda tympani, mandibular nerve and its branches, middle meningeal artery, pterygoid venous plexus and retromandibular vein, inferior part of temporalis, medial and lateral pterygoids, and deep lobe of the parotid gland [10]. Furthermore, it communicates with a number of important anatomical regions, including the pterygopalatine fossa, middle cranial fossa, and orbit [3].

Due to its complex anatomy and deep location, visualization of the infratemporal fossa can be challenging [21]. The intricate micro-neurovascular anatomy of the region has been thoroughly documented [9, 10]; nevertheless, the distances between the bony borders have not been thoroughly investigated. It is essential to appreciate the anatomical boundaries and integrity of this region in order to improve the understanding of the complex nature of the infratemporal fossa and its relevance in a variety of disciplines, ranging from surgical interventions to curriculum development and training courses [3, 20].

Following the creation of three dimensional (3D) anatomical models from computed tomography (CT) images in 1979, significant technological advances have enabled such models to be widely used in medical applications [1, 16]. Due to the complexity and inaccessability of regions such as the infratemporal fossa, it is inherently difficult to obtain measurements in cadavers or from dry bones. Reconstructed 3D digital models provide the most effective tools for evaluating such complex areas [18].

A detailed 3D morphometric analysis of the infratemporal fossa can be used to quantify the distances between its bony borders, thereby filling an important gap in the literature. Such analysis can be undertaken using 3D

reconstructions of the infratemporal fossa and provide a comprehensive overview of the anatomical integrity of the region.

The current study focused on exploring the 3D morphometric relationships between the bony margins of the infratemporal fossa. Models were reconstructed from Digital Imaging and Communications in Medicine (DICOM) datasets, to provide an accurate 3D representation of the anatomy of the infratemporal fossa. Determination of the distances (length, depth, width) between the bony margins of the infratemporal fossa was accomplished using 3D imaging techniques.

Materials and methods

Data source

Axial CT images of patients screened between January 2021 and January 2022 constituted the data source for the study. Cranial CT images were randomly selected from the archive of the Radiology Department, Faculty of Medicine, Cukurova University. This was a retrospective study which recieved institutional review board approval (Protocol no: 6.12.2019/94-18). All scans were obtained using a 160-slice MDCT scanner (Toshiba Aquilion™ PRIME; Otawara, Japan) with the following standard protocol: 0.6 mm collimation with 0.5 mm slice thickness, 120 kV, and 250 m. The images (0.5 mm axial sections and 3D reformatted) were evaluated using a bone window setting (Width: 2500; Level:500) and a digital workstation (Vitrea CT workstation, Toshiba; Otawara, Japan). One hundred and eighteen (118) CT images were initially selected; however, after applying exclusion criteria (trauma, tumors, previous cranial surgery, degenerative changes, temporomandibular joint-TMJ disorders, images of patients with dental implants and those with incomplete images) this left 83 DICOM datasets for use in the study: these were subsequently anonymized and analysed.

Segmentation and measurements

Segmentation of the 3D models was conducted using *3D Slicer*, an open source software platform. The DICOM datasets for each patient were imported and visualized using a bone preset algorithm in the *Volume Rendering Module*. Borders of the infratemporal fossa were determined using the *Region of Interest (ROI)* tool: the 3D models were cropped using the *Crop Volume Module*. The cropped series were then segmented using the *Segment Editor Module*. Morphometric parameters (length, depth, width) were measured using the *Markups Module*, and the results recorded in an external Excel document. The following distances were determined:

- **Length:** Between the posterior wall of the maxillary sinus anteriorly and the deepest point on the anterior surface of the styloid process posteriorly. The anterior landmark was taken as the deepest point which was cut through by a horizontal plane tangential to the superior surface of the zygomatic arch (Fig. 1A and Fig. 2).
- **Depth:** Between the infratemporal crest superiorly and the attachment area of medial pterygoid on the angle of the mandible inferiorly. The inferior landmark was determined on the segmentation process by adding guide points to the attachment area of medial pterygoid (Fig. 1B and Fig. 3).
- **Width:** Between the most superior point of the pterygoid process medially and the medial surface of the deepest point of the mandibular notch laterally. The medial landmark was determined as the midpoint of the line where the lateral pterygoid process descends from the junction of the body and greater wing of the sphenoid (Fig. 1C).

In accordance with ethical and scientific guidelines, a single examiner provided informed consent for the publication of representative images generated from the CT scans. These images exemplify the parameters of the study and provide a visual representation of the data collected.

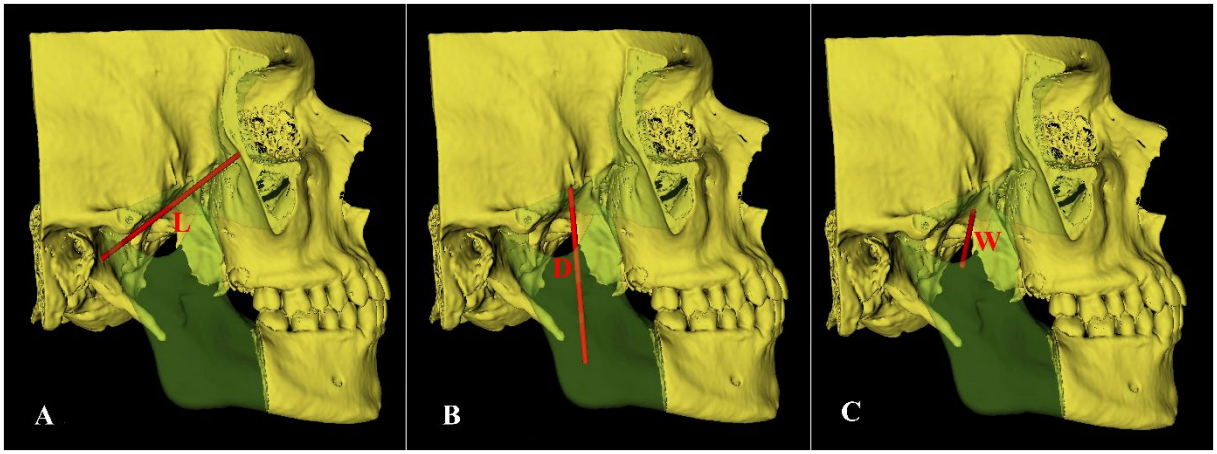

Fig. 1. Morphometric measurements of the bony boundaries of the infratemporal fossa. The opacity of the mandibular ramus and the zygomatic arch was digitally adjusted to 35%, thereby allowing the visualization of anatomical landmarks. **A.** Length (L), **B.** Depth (D) and **C.** Width (W) of the infratemporal fossa.

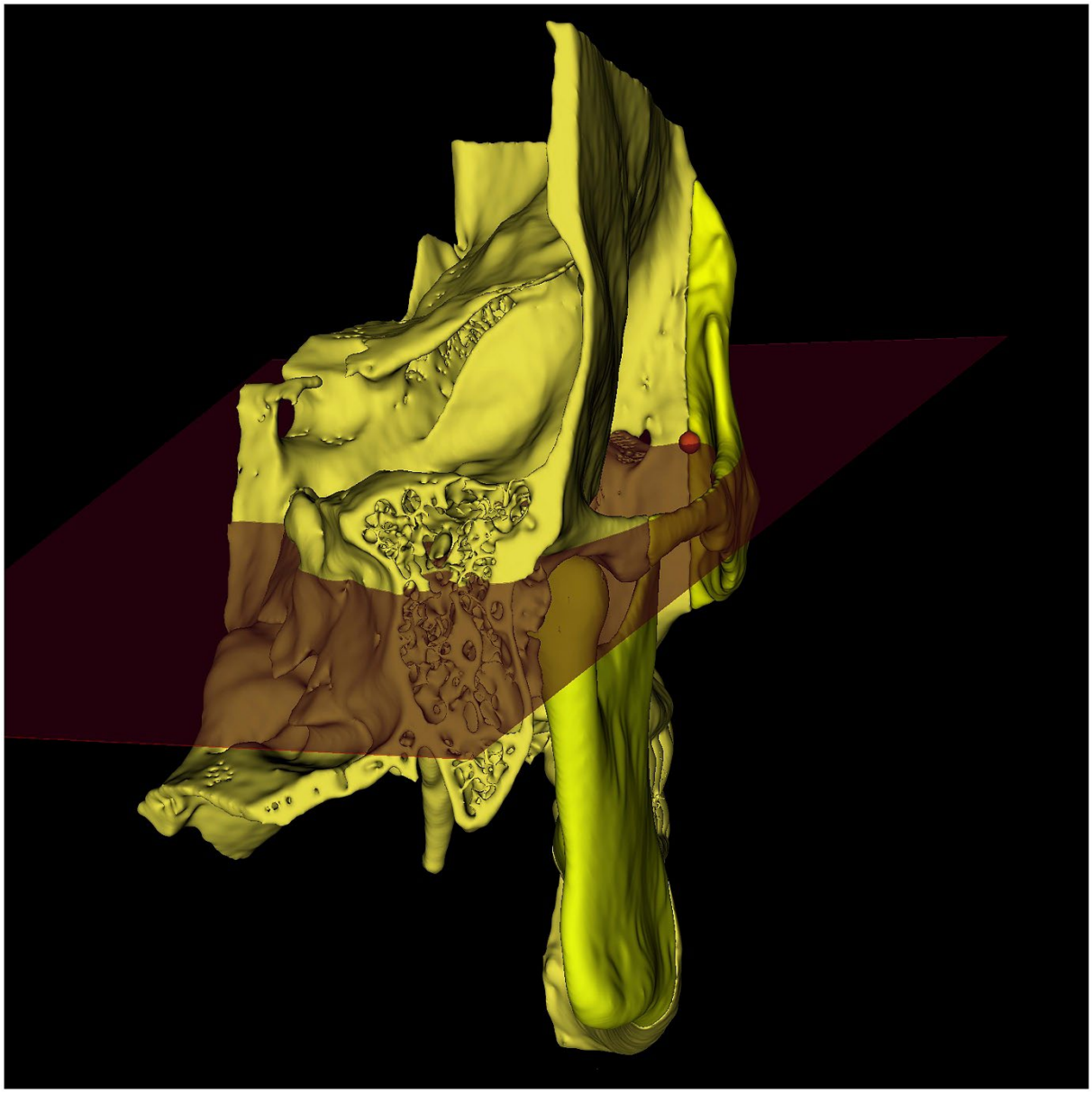

Fig. 2. The anterior border of the infratemporal fossa can be visualized from a posterolateral view: the red dot indicates the anterior border of the infratemporal fossa.

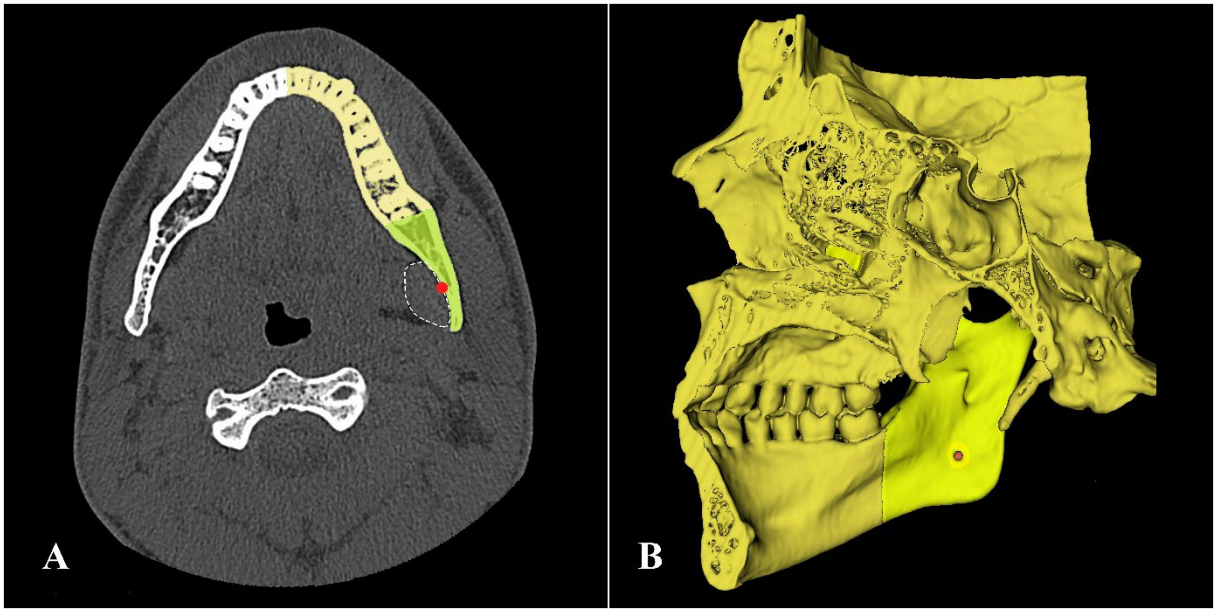

Fig. 3. Determination of the attachment of lateral pterygoid in the segmentation process and its appearance in the 3D digital model. **A.** The dashed line surrounds medial pterygoid. A digitally-generated red dot was utilized to depict the inferior landmark of the depth (D) measurement. **B.** Segmented 3D model showing the inferior landmark (red dot) of the depth (D) measurement viewed medially.

Statistical analysis

All statistical analyses were performed using IBM SPSS Statistics Version 20.0 statistical software package (SPSS Inc., Chicago, IL, USA). Continuous variables were summarized as means and standard deviations. The Kolmogorov-Smirnov test was used to analyze the distribution of each dataset into parametric and nonparametric data. For comparison of continuous variables between two groups, the Student's t-test was used. Correlations between each pair of dimensions (length, depth and width) for each side and between sides were analyzed using the Pearson r correlation. Intra-observer reliability was analysed by means of intra-class correlation coefficients (ICC). P-values <0.05 were considered to be statistically significant.

Results

The intraclass corelation coefficients (ICC) for each of the measurements taken from the datasets are shown in Table 1. According to the evaluation of Koo & Li (2016) the intraobserver reliability of repeated measures were good and excellent [13].

Table 1 Intra-observer reproducibility and reliability for each the measurements taken.

Parameters	ICC (95% CI)	p
Left Length	0.887 (0.812-0.932)	**<0.001**
Left Depth	0.941 (0.902-0.965)	**<0.001**
Left Width	0.854 (0.756-0.912)	**<0.001**
Right Length	0.906 (0.843-0.944)	**<0.001**
Right Depth	0.913 (0.855-0.948)	**<0.001**
Right Width	0.920 (0.867-0.952)	**<0.001**

ICC: Intraclass Correlation Coefficient, CI: confidence interval

From the DICOM datasets of 83 patients included in the study (40 males, 43 females), the average age was 47.8±20.8 years (male: 48.5±20.9; female: 47.2±20.9) with a range of 9 to 82 years: no significant differences (p=0.764) in age was observed between males and females. However, all measurements were significantly different between males and females (Table 2), with males having the greater values. While there was no significant difference between the left and right sides for length, significant differences were observed for depth and width (Table 3). There were moderate positive correlations between age and both left and right width measurements (Table 4), with the strongest being between age and width for each side. There were moderate positive correlations between each pair of dimensions (length, depth and width) for each side. Not surprisingly, high positive correlations were observed between the same parameters on the left and right sides (Table 4).

Table 2 The mean, standard deviation (SD) and range of the length, depth and width (mm) of the infratemporal fossa in males and females.

Parameters	**Male**	**Female**	
	Mean ± SD (Range)	**Mean ± SD (Range)**	**P-value**
Length	61.1 ± 4.4 (47.6 - 68.9)	59.1 ± 3.3 (64.4 - 51.3)	0.019*
Depth	60.1 ± 4.4 (47.3 - 66.7)	52.2 ± 3.7 (60.5 - 44.9)	<0.001*
Width	28.2 ± 4.0 (33.8 – 18.0)	26.1 ± 2.8 (32.9 – 20.0)	0.007*

*Student's t test

Table 3 Comprasion between the left and right side lengths, depths and widths (mm) for the complete dataset.

Parameters		**Left Side**	**Right Side**		
	n	**Mean ± SD (Range)**	**Mean ± SD (Range)**	**r**	**P-value**
Length	83	60.3 ± 4.2 (48.5 – 71.0)	59.8 ± 4.2 (46.7 – 68.2)	0.855	0.089
Depth	61	55.4 ± 6.0 (43.8 – 69.0)	56.0 ± 6.7 (32.8 – 68.3)	0.837	0.008*
Width	80	26.9 ± 3.7 (18.5 – 34.9)	27.3 ± 3.7 (17.4 – 34.8)	0.883	0.020*

SD: standard deviation; r: Paired Samples Correlations; *Paired samples t test

Table 4 Pearson correlation coefficients (r) between pairs of parameters (length, depth and width) for each side and between the left and right sides.

	Left	**Right**

		Length	Depth	Width	Length	Depth	Width
	Age	0.159	0.249	0.570**	0.265*	0.177	0.547**
Left	**Length**		0.424**	0.383**	0.855**	0.410**	0.451**
	Depth			0.433**	0.515**	0.837**	0.542**
	Width				0.418**	0.397**	0.883**
Right	**Length**					0.423**	0.503**
	Depth						0.541**

* Correlation is significant at the 0.05 level (2-tailed).

** Correlation is significant at the 0.01 level (2-tailed).

Discussion

In the current study, 3D models of the skull were reconstructed from the DICOM datasets of 83 patients, from which the distances between the bony borders of the infratemporal fossa were determined. Although there were specific exclusion criteria, age was not one of them as lesions involving the infratemporal fossa are not age dependent. The length, depth and width measurement were taken for each side (left, right) and evaluated (Table 3). The main scope of the study was to define the anatomical extent of the infratemporal fossa.

A significant difference between the left and right sides in terms of depth and width, but not length, was observed. This could be attributed to the functions of the muscles involved in mastication. Wolff's law postulates a relationship between the morphology of the bones and the function of adjacent muscles [28]. Physical stresses, such as those produced by muscles involved in mastication, could influence the shape of bones [19, 25]. The precise mechanism by which mastication influences craniofacial bone growth is unclear; however, this effect may be related to the capacity of masticatory muscles [2]. Moreover, since mastication is mostly performed on the dominant side of the jaw, bilateral asymmetry of the mandible would be expected [12, 29].

Cranial bone pathology, such as trauma or neoplasms, can significantly alter the skeletal anatomy and have a detrimental impact on quality of life [11]. In such cases autologous bone allografts are the optimal and preferred method for the bony reconstruction. However when there is a large skull defect with concurrent autologous bone resorption, allografts alone may not provide adequate protective and aesthetic results [23]. The use of Computer-Aided Design (CAD) software and patient-specific DICOM files to model 3D printed prostheses is a relatively safe procedure that has few complications [4]. In the fabrication of 3D-printed cranial prostheses for unilateral defects, the contralateral side is used as a mirror image to generate the appropriate 3D model [5]. Bilateral symmetry/asymmetry in cranial bones is a significant factor to take into consideration when fabricating 3D-printed prostheses [15]. The current study revealed strong correlations between the length, depth and width measurements of the right and left sides. This confirms that the contralateral side can be used to reconstruct 3D printed prostheses of the cranium (and skull) of the injured/damaged side in preoperative diagnosis, planning, and surgical practice.

Medical image data, specifically CT and MRI scans, are used to create high-resolution anatomically accurate 3D models for research, surgical planning, educational and training purposes. These models are widely used in morphometric studies through virtual quantitative analyses [16]. Traditionally, caliper methodologies have been , and are, used in morphometric analysis: it is extremely challenging to undertake morphometric analyses using these methods in areas with narrow and complex shapes, such as the infratemporal fossa [1]. With traditional

morphometric methods, the process of obtaining useful measurements is extremely time-consuming procedure [17]. Furthermore, traditional methods may lead to subjective reporting, and possibly inaccurate measurements, which may lead to inaccurate manipulation in neurovascular surgery [26].

The use of 3D digital anatomical models in scientific studies has become more common. With the widespread use of such models, there has also been an increase in 3D reconstruction softwares. The softwares available differ from each other in terms of technical capabilities and cost-effectiveness [16]. 3D Slicer is a free, open source software for creating 3D reconstructions from a variety of image formats, including DICOM datasets. It has a functional graphic user interface: its functionality can be enhanced with extensions that can be used for a multitude of scientific purposes [30]. In the current study, 3D models were readily reconstructed and useful morphometric measurements obtained. Moreover, futuristic and yet simple visual images were obtained.

Variations in the morphology of the infratemporal fossa must be taken into consideration when planning for surgery in the region [6]. Most anatomic descriptions relating to the infratemporal fossa refer to its microsurgical anatomy [9, 10, 22, 27]. However, from a macro (gross) anatomical perspective it is surprising that landmarks and/or the distances between the bony boundaries of the infratemporal fossa have not been reported. The current study showed significant differences in length, depth and width between males and females, with all measurements being significantly greater in males. These differences need to be taken into account when planning surgical interventions in the regoin, as they may impact the outcome of the procedure.

Infratemporal fossa tumors are rare clinical phenomena, with epidemiological knowledge being insufficient to understand the pathology in all its aspects. It is difficult to distinguish between benign or malign tumors in the fossa by routine examination. Differential diagnosis of pathologies such as neoplastic formations, aneurysms and atherosclerosis are based on radiographic (CT, MRI) images and physical examination [24]. Exploration of the region during radical surgery is restricted due to the presence of delicate neurovascular structures [6]. However, with the widespread use of endoscopic imaging modalities, a number of surgical techniques have been developed [7, 8, 14]. On the other hand, a detailed 3D anatomical representation is imperative in the management of lesions in the infratemporal fossa to prevent potentially serious postoperative complications [9].

Limitations of the study

The results of the current study should be viewed in the context of its limitations. Firstly, the study was limited by its retrospective design and did not include a comparison of the measurements obtained with rapid prototyped models, dry skull bones, or cadaveric material. As such, the results may not be generalizable to other study designs. Secondly, the sample size was relatively small: further studies with larger sample sizes are needed to confirm the study observations. Finally, the sample used in the study was obtained from a single center and may not be representative of the general population. Again, further studies with larger and more diverse sample populations are needed to better understand the influence of gender and/or age on infratemporal fossa dimensions.

Conclusion

To the best of our knowledge, this is the first study that documents the distances (length, depth, width) between the bony boundaries of the infratemporal fossa. Clear determination of the definitions and landmarks used are essential for a standardized examination of the region. In order to obtain standardized results, an attempt was

made to use easily identifiable landmarks. It is anticipated that these landmarks can be used by others to determine the morphometric and morphological characteristics of the infratemporal fossa between different ethnic groups and/or races. It is hoped that future research will support or challenge the results reported in this study, ultimately leading to the establishment of a comprehensive and reliable database of the dimensions of the infratemporal fossa.

Funding

This research did not receive any specific grant from funding agencies in the public, commercial, or not-for-profit sectors.

Competing interests

The authors have no relevant financial or non-financial interests to disclose.

Conflict of interest

All authors declare that they have no conflict of interest.

Ethics approval

Ethical approval was waived by the local Ethics Committee of Cukurova University in view of the retrospective nature of the study and all the procedures being performed were part of the routine care (Protocol no: 6.12.2019/94-18).

Authors' contributions

Conceptualization: [Huseyin Erdem], [Neslihan Boyan], [Ozkan Oguz]; Methodology: [Huseyin Erdem], [Ozkan Oguz]; Formal analysis and investigation: [Huseyin Erdem], [Nazire Kilic Safak]; Writing - original draft preparation: [Huseyin Erdem]; Writing - review and editing: [Huseyin Erdem], [Yigit Cevik], [Roger Soames]; Resources: [Umur Anil Pehlivan]; Supervision: [Ozkan Oguz], [Neslihan Boyan]; Visualization: [Yigit Cevik], [Huseyin Erdem]

References

1. Adams GL, Gansky SA, Miller AJ, Harrell WE, Jr., Hatcher DC (2004) Comparison between traditional 2-dimensional cephalometry and a 3-dimensional approach on human dry skulls. Am J Orthod Dentofacial Orthop 126(4): 397-409. https://doi.org/10.1016/j.ajodo.2004.03.023
2. Boom HP, van Spronsen PH, van Ginkel FC, van Schijndel RA, Castelijns JA, Tuinzing DB (2008) A comparison of human jaw muscle cross-sectional area and volume in long- and short-face subjects, using MRI. Arch Oral Biol 53(3): 273-281. https://doi.org/10.1016/j.archoralbio.2007.08.013
3. Casale J, Bordoni B, Anatomy, head and neck, infratemporal fossa, in Statpearls. 2022: Treasure Island (FL). https://www.ncbi.nlm.nih.gov/books/NBK537034/. Accessed 20 Feb 2023.
4. De La Pena A, De La Pena-Brambila J, Perez-De La Torre J, Ochoa M, Gallardo GJ (2018) Low-cost customized cranioplasty using a 3D digital printing model: A case report. 3D Print Med 4(1): 4. https://doi.org/10.1186/s41205-018-0026-7

5. Dumas BM, Nava A, Law HZ, Smartt J, Derderian C, Seaward JR, Kane AA, Hallac RR (2019) Three-dimensional printing for craniofacial surgery: A single institution's 5-year experience. Cleft Palate Craniofac J 56(6): 729-734. https://doi.org/10.1177/1055665618798292
6. Dwivedi G, Gupta V, Tiwari V, Patnaik U, Sood A, Kumari A, Bharadwaja S (2022) Different approaches to the overlapping infratemporal fossa and parapharyngeal spaces: A case series and review of literature. Indian J Otolaryngol Head Neck Surg 74(Suppl 2): 2337-2343. https://doi.org/10.1007/s12070-020-02168-2
7. Gao L, Zhou L, Dai Z, Huang X (2017) The endoscopic prelacrimal recess approach to the pterygopalatine fossa and infratemporal fossa. J Craniofac Surg 28(6): 1589-1593. https://doi.org/10.1097/SCS.0000000000003419
8. Hosseini SM, Razfar A, Carrau RL, Prevedello DM, Fernandez-Miranda J, Zanation A, Kassam AB (2012) Endonasal transpterygoid approach to the infratemporal fossa: Correlation of endoscopic and multiplanar CT anatomy. Head Neck 34(3): 313-320. https://doi.org/10.1002/hed.21725
9. Isolan GR, Rowe R, Al-Mefty O (2007) Microanatomy and surgical approaches to the infratemporal fossa: An anaglyphic three-dimensional stereoscopic printing study. Skull Base 17(5): 285-302. https://doi.org/10.1055/s-2007-985193
10. Joo W, Funaki T, Yoshioka F, Rhoton AL, Jr. (2013) Microsurgical anatomy of the infratemporal fossa. Clin Anat 26(4): 455-469. https://doi.org/10.1002/ca.22202
11. Kelly RR, Sidles SJ, LaRue AC (2020) Effects of neurological disorders on bone health. Front Psychol 11: 612366. https://doi.org/10.3389/fpsyg.2020.612366
12. Kim TH, Kim CH (2020) Correlation between mandibular morphology and masticatory muscle thickness in normal occlusion and mandibular prognathism. J Korean Assoc Oral Maxillofac Surg 46(5): 313-320. https://doi.org/10.5125/jkaoms.2020.46.5.313
13. Koo TK, Li MY (2016) A guideline of selecting and reporting intraclass correlation coefficients for reliability research. J Chiropr Med 15(2): 155-163. https://doi.org/10.1016/j.jcm.2016.02.012
14. Li L, London NR, Jr., Prevedello DM, Carrau RL (2022) Endoscopic endonasal approach to the pterygopalatine fossa and infratemporal fossa: Comparison of the prelacrimal and denker's corridors. Am J Rhinol Allergy 36(5): 599-606. https://doi.org/10.1177/19458924221097159
15. Lim HK, Choi YJ, Choi WC, Song IS, Lee UL (2022) Reconstruction of maxillofacial bone defects using patient-specific long-lasting titanium implants. Sci Rep 12(1): 7538. https://doi.org/10.1038/s41598-022-11200-0
16. Martin CM, Roach VA, Nguyen N, Rice CL, Wilson TD (2013) Comparison of 3D reconstructive technologies used for morphometric research and the translation of knowledge using a decision matrix. Anat Sci Educ 6(6): 393-403. https://doi.org/10.1002/ase.1367
17. Motoike HK, O'Kane RL, Lenchner E, Haspel C (2009) Clay modeling as a method to learn human muscles: A community college study. Anat Sci Educ 2(1): 19-23. https://doi.org/10.1002/ase.61
18. Murgitroyd E, Madurska M, Gonzalez J, Watson A (2015) 3D digital anatomy modelling - practical or pretty? Surgeon 13(3): 177-80. https://doi.org/10.1016/j.surge.2014.10.007

19. Pepicelli A, Woods M, Briggs C (2005) The mandibular muscles and their importance in orthodontics: A contemporary review. Am J Orthod Dentofacial Orthop 128(6): 774-780. https://doi.org/10.1016/j.ajodo.2004.09.023
20. Prades JM, Timoshenko A, Merzougui N, Martin C (2003) A cadaveric study of a combined trans-mandibular and trans-zygomatic approach to the infratemporal fossa. Surg Radiol Anat 25(3-4): 180-187. https://doi.org/10.1007/s00276-003-0126-x
21. Roche PH, Fournier HD, Laccourreye L, Mercier P (2001) Surgical anatomy of the infratemporal fossa using the transmaxillary approach. Surg Radiol Anat 23(4): 209-213. https://doi.org/10.1007/s00276-001-0209-5
22. Rusu MC, Pop F, Curca GC, Podoleanu L, Voinea LM (2009) The pterygopalatine ganglion in humans: A morphological study. Ann Anat 191(2): 196-202. https://doi.org/10.1016/j.aanat.2008.09.008
23. Tessier P, Kawamoto H, Matthews D, Posnick J, Raulo Y, Tulasne JF, Wolfe SA (2005) Autogenous bone grafts and bone substitutes--tools and techniques: I. A 20,000-case experience in maxillofacial and craniofacial surgery. Plast Reconstr Surg 116(5 Suppl): 6S-24S. https://doi.org/10.1097/01.prs.0000173862.20563.12
24. Tiwari R, Quak J, Egeler S, Smeele L, Waal IV, Valk PV, Leemans R (2000) Tumors of the infratemporal fossa. Skull Base Surg 10(1): 1-9. https://doi.org/10.1055/s-2000-6789
25. Toro-Ibacache V, Zapata Munoz V, O'Higgins P (2016) The relationship between skull morphology, masticatory muscle force and cranial skeletal deformation during biting. Ann Anat 203: 59-68. https://doi.org/10.1016/j.aanat.2015.03.002
26. van Vlijmen OJ, Maal T, Berge SJ, Bronkhorst EM, Katsaros C, Kuijpers-Jagtman AM (2010) A comparison between 2D and 3D cephalometry on cbct scans of human skulls. Int J Oral Maxillofac Surg 39(2): 156-160. https://doi.org/10.1016/j.ijom.2009.11.017
27. Vrionis FD, Cano WG, Heilman CB (1996) Microsurgical anatomy of the infratemporal fossa as viewed laterally and superiorly. Neurosurgery 39(4): 777-786. https://doi.org/10.1097/00006123-199610000-00027
28. Weijs WA, Hillen B (1984) Relationships between masticatory muscle cross-section and skull shape. J Dent Res 63(9): 1154-1157. https://doi.org/10.1177/00220345840630091201
29. Witzel U, Preuschoft H (2002) Function-dependent shape characteristics of the human skull. Anthropol Anz 60(2): 113-135. https://doi.org/10.1127/anthranz/60/2002/113
30. You Y, Niu Y, Sun F, Huang S, Ding P, Wang X, Zhang X, Zhang J (2022) Three-dimensional printing and 3D Slicer powerful tools in understanding and treating neurosurgical diseases. Front Surg 9: 1030081. https://doi.org/10.3389/fsurg.2022.1030081